

TECH. MEMO  
AERO 2159

DTIC FILE COPY

UNLIMITED

(2)

BR112416

TECH. MEMO  
AERO 2159



ROYAL AEROSPACE ESTABLISHMENT

AD-A218 227

DTIC  
ELECTE  
FEB 21 1990  
S D

USE OF LIQUID CRYSTALS FOR QUALITATIVE AND QUANTITATIVE 2-D STUDIES  
OF TRANSITION AND SKIN FRICTION

by

L. Gaudet

T. G. Gell

Original contains color  
plates. DTIC reproduction  
will be in black and  
white.

June 1989

DISTRIBUTION STATEMENT A  
Approved for public release  
Distribution Unlimited

Procurement Executive, Ministry of Defence  
Farnborough, Hampshire

90 02 20 033

UNLIMITED

0058658

CONDITIONS OF RELEASE

BR-112416

\*\*\*\*\*

U

COPYRIGHT (c)  
1988  
CONTROLLER  
HMSO LONDON

\*\*\*\*\*

Y

Reports quoted are not necessarily available to members of the public or to commercial organisations.

UNLIMITED

R O Y A L   A E R O S P A C E   E S T A B L I S H M E N T

Technical Memorandum Aero 2159

Received for printing 15 June 1989

USE OF LIQUID CRYSTALS FOR QUALITATIVE AND QUANTITATIVE 2-D STUDIES  
OF TRANSITION AND SKIN FRICTION

by

L. Gaudet

T. G. Gell

SUMMARY

The exploitation of the properties of liquid crystals for use in wind tunnels to visualise transition and to measure skin friction is described. The effectiveness of a transition band to trip the laminar boundary layer on a swept wing is demonstrated by the growth of turbulent wedges with Reynolds number.

The ability of liquid crystals to reveal intricate surface flow structure is clearly shown by subtle changes of colour on an unswept rectangular wing when subjected to the combined effects of transition, separation, reattachment and a normal shock. The time response of liquid crystals to changes in shear stress is illustrated by the shock pattern on the model surface which was seen to be oscillating.

A method involving the digitisation of the video image into its three component colours has the potential for measuring skin friction in great detail. This involves using relationships firstly correlating the component colours with wavelength and secondly correlating shear stress with wavelength. *G. N. + Sp...*

*Paper prepared for ICIASF '89 DLR Göttingen 18-21 September 1989*

*Copyright*

©

*Controller HMSO London*

*1989*

*1*

LIST OF CONTENTS

	<u>Page</u>
1 INTRODUCTION	3
2 PROPERTIES OF LIQUID CRYSTALS	4
3 MODES OF USE	5
3.1 Temperature measurement	5
3.2 Mixed temperature and shear stress mode	6
3.3 Shear stress mode	6
4 RESULTS	7
4.1 Mixed mode results	7
4.1.1 Forced transition on a swept wing	7
4.1.2 Laminar separation bubble on stub wing	8
4.2 Results in shear stress mode	8
4.2.1 Stub wing	8
4.2.2 Swept wing - transition free	9
4.2.3 Swept fin - transition fixed	10
4.2.4 Swept wing - isolated roughness	10
5 QUANTITATIVE ASPECTS	11
6 DISCUSSION	12
7 CONCLUSIONS	14
References	15
Illustrations	Figures 1-19
Report documentation page	inside back cover



Accession For:	
NTIS CRA&I	<input checked="" type="checkbox"/>
DTIC TAB	<input type="checkbox"/>
Unannounced	<input type="checkbox"/>
Justification:	
By	
Distribution/	
Availability Codes	
Dist	
A-1	

## 1. INTRODUCTION

With the need to develop aircraft of high performance combined with maximum efficiency it is becoming increasingly important that the transition from laminar to turbulent boundary layer flow on wind tunnel models is well defined. On the one hand, the visualisation of natural transition is useful for confirming, or otherwise, design techniques with the aim of increasing the area of laminar flow over wings in order to reduce the overall skin-friction drag. On the other hand, to simulate flight Reynolds number in the wind tunnel, it is often necessary to ensure that the boundary layer is turbulent and that its thickness scales correctly. To achieve the latter requirements, transition bands are employed in appropriate positions to cause the approaching laminar boundary layer to become turbulent. The trip must be effective in ensuring the boundary layer is fully turbulent just downstream of it without excessive thickening (overfixing). Ideally in order to ensure that these conditions are satisfied it is desirable that the transition process be viewed as the test conditions are approached.

The prime interest in using liquid crystals at RAE has been to find an alternative to oil flow, sublimation and thermal imaging techniques for verifying transition mainly on steel wind tunnel models. The main advantages, compared with oil flow and sublimation techniques, is that the crystal response is reversible so that continuous on-line assessment of the flow conditions is possible for a single application of liquid crystals. Since liquid crystals can be chosen to respond to shear by change of colour the sharp wedges of turbulence can be easily observed. Transition is normally less well defined when employing techniques relying on the surface temperature change across the transition boundary due to heat conduction in the surface of the metal model (unless it is thermally insulated). Since the gradation of colour is an indication of the shear stress level it is possible to quantify the skin friction levels over a model surface by the use of a video digitisation process and a shear stress calibration.

RAE interest in the use of liquid crystals for surface-flow visualisation was initially stimulated by a NASA, Langley report [1] showing a colour photograph of transition visualisation in flight on the winglet of a Gates Learjet business transport aeroplane at  $M = 0.8$  and an altitude of  $\approx 15000$  m .

## 2. PROPERTIES OF LIQUID CRYSTALS

Liquid crystals are optically active mixtures of organic compounds which have the ability to reflect light of a particular wavelength which changes in response to certain physical stimuli. These stimuli include temperature, shear stress, pressure, magnetic and electric fields etc. In wind tunnel testing involving the investigation of the surface flow over models the two stimuli of interest are temperature and shear stress and the discussion will be limited to these.

Liquid crystals, as their name implies, are substances which exhibit crystalline type properties while still remaining in a liquid state. They have consistencies varying from that similar to a motor oil ( $\approx 0.05 \text{ NS/m}^2$ ) to that of a viscous paste. Chiral nematics, the least viscous form of liquid crystals, are produced synthetically while the more viscous material consists of cholesterol esters which are found naturally in the form of fatty acids etc.

The investigations at RAE have been concerned mainly with the use of chiral nematics since they have a high response rate and the required film thickness on a model is small - being typically  $10 \mu\text{m}$ . A phase diagram for these liquid crystals is shown in Fig 1a for a range of crystal formulations. In the smectic phase, which is closest to the crystal phase, the crystal structure is well organised and in its simplest form may consist of layers of molecules parallel with one another. In response to a stimulus such as temperature the regular layers are disturbed and the molecular distribution is more random but with the long axes of the molecules remaining substantially parallel. This is the nematic phase. Further increase in temperature will 'melt' the liquid crystal into the isotropic phase.

It is the special classification of nematics known as chiral nematics which is of particular interest. Chiral nematics consist of layers of molecular structures, one upon the other, whose physical properties rotate from one layer to the next forming a helical type structure. Optically, these materials are highly active with optical rotations in the range of  $10^3 - 10^5$  degrees per mm for visible light [2].

When viewed with white light, the wavelength  $\lambda_0$  of the reflective light is related to the pitch  $p$  of the helix and the mean refractive index  $n$  by

$$\lambda_0 = np$$

when viewed normally. When viewed obliquely a change in wavelength occurs since the material acts as a three-dimensional diffraction grating and exhibits characteristics similar to those associated with Bragg scattering.

If, however, the liquid crystal in the nematic phase on a surface is undisturbed, a colourless focal conic texture may result with the helical structures out of phase with the incident light. Application of a shear stress will orientate the liquid crystals to produce a Grandjean texture with the helical structures perpendicular to the surface as illustrated in Fig 1b. This is the texture which produces the bright colours normally associated with liquid crystals. Since the pitch of the helix and hence the wavelength of the reflected light are influenced by temperature (and shear stress), the colour exhibited by the liquid crystal systematically follows the visual colour spectrum. It is usual for the colour scale to start at red and pass through the spectrum to blue with increasing stimulus.

However, since chiral nematics contain up to 10 organic substances, it is possible to arrange the mixtures to reverse the colour order or arrange the colour display to start at a specific point in the spectrum. It is also possible to suppress the response to temperature while retaining the sensitivity to shear stress, thus providing a shear-stress-only liquid crystal.

### 3. MODES OF USE

Liquid crystals may be used in three modes each having its own advantages. These modes are temperature, shear stress and the combination of the two. While there is considerable interest in the temperature aspect especially in relation to heat transfer [3,4], the main interest at RAE has centred on the shear stress response for transition detection and the experimental data relates to this aspect.

#### 3.1 Temperature measurement

Micro encapsulation in polymer shells allows the 'neat' (unencapsulated) liquid crystal to be insensitive to shear stress and therefore to be solely temperature sensitive. The micro-encapsulated liquid crystals vary in size, being typically of 8-15  $\mu\text{m}$  diameter and need to be mixed with a binder so that they may be sprayed or painted onto the surface: experience suggests that the layer should be about 30  $\mu\text{m}$  thick. The process of encapsulation produces a Grandjean texture ensuring that colours are always visible within the temperature bandwidth of the liquid crystal. The temperature profile of a liquid crystal is



#### 4. RESULTS

Most of the results have been obtained in the 2ft x 1½ft Transonic Wind Tunnel at RAE Farnborough. Figs 4 and 5 illustrate the test arrangement. The models were mounted on a turntable in the roof of the working section. The models were illuminated by Quartz-Halogen lamps positioned in the plenum chamber to produce optimum illumination of the model surface without glare. Photography was by means of both a video camera and a still camera positioned outside of the tunnel shell. In later tests, two lamps (1200 W each) were employed to improve the illumination (one upstream and one downstream of the model).

Because of the restriction of the working section window some shadows occur in the photographs. In addition an out-of-focus image of the sidewall slots (including the corrugated resistance elements) will be apparent in all views.

##### 4.1 Mixed mode results

###### 4.1.1 Forced transition on a swept wing\*

Fig 6 shows the increasing effectiveness of a transition trip on a swept wing, formed with ballotini at 10% chord, with increasing Reynolds number. The wing was painted matt-black downstream of 15% chord. A layer of liquid crystal R20C15W was sprayed onto the surface. The model was illuminated and photographed in a position directly above model. The tunnel speed was increased at atmospheric pressure until the Reynolds number was  $Re_c^- = 1.2 \times 10^6$  and the Mach number was 0.2 with the total temperature  $T_0 = 17^\circ\text{C}$ . At these conditions there is no colour response due to the low temperature and the liquid crystal is initially in the smectic phase. With the development of turbulence from the transition trip with increase of Reynolds number, the liquid crystals are driven into the nematic phase to produce a Grandjean texture. The turbulence is seen as wedges of orange and yellow. With increase of Reynolds number the number of turbulent wedges increases until the area downstream of the transition trip is fully turbulent. This experiment illustrates the usefulness of this mode for confirmation of transition fixing provided the liquid crystal and test conditions are matched.

---

\* ARA Ltd, Manton Lane, Bedford, kindly permitted RAE to obtain these results in their large Transonic Tunnel.

#### 4.1.2 Laminar separation bubble on stub wing

Fig 7 shows the flow over a 15% thick section rectangular wing (referred to as a stub wing for convenience hereafter) with chord  $c = 102$  mm and span 178 mm. A transition trip of 3 mm streamwise width consisting of glass spheres (or ballotini) of 0.127 mm diameter was placed at 15% chord from the leading edge as shown in Fig 7. The test Reynolds number was  $Re_{\bar{c}} = 3.4 \times 10^5$  at  $M = 0.5$  and all the results shown here are for zero angle of incidence ( $\alpha = 0^\circ$ ). The surface was sprayed with liquid crystal specification R15C20W downstream of the transition trip. Initially, only the matt black background was visible. Generally the transition trip was ineffective at the test conditions and a laminar separation bubble developed at the half chord position. The shear stress in the bubble region is too small to activate the liquid crystal into a Grandjean texture so leaving a neutral focal conic texture with the matt black surface showing through. Downstream of the transition trip the colour changes from green to orange indicating a reduction in shear stress. The edge of the black zone is tinged with orange indicating the low shear stress at separation. Reattachment of the boundary layer immediately downstream of the bubble is indicated by a black line. A flow region of high shear stress (green) is observed in the reverse flow regions immediately upstream of reattachment, shear stress reducing further upstream (orange) to a region of negligible shear stress (black). Two wedges of turbulence, generated by individual roughness elements, can be seen to have penetrated the bubble and activated the liquid crystals in the region.

#### 4.2 Results in shear stress mode

##### 4.2.1 Stub wing

Use of liquid crystals in the shear stress mode allows very fine detail of the flow to be viewed. Fig 8a is a view similar to Fig 7 but at  $M = 0.25$ ,  $Re_{\bar{c}} = 5 \times 10^5$  and the development of turbulent wedges from the transition trip is increased. The wedges break up the laminar bubble and subtle gradations of colour are apparent. The turbulent wedges are green with a background of laminar flow (orange). Under the bubble there are areas of red where the liquid crystal has been activated by a turbulent vortex structure and presumably the vortex has lifted from the surface to leave a Grandjean texture indicating a low shear stress. The nature of the generation of the turbulence from the individual elements in the transition trip is illustrated in Fig 8b which is an enlargement from Fig 8a. It is seen that the turbulent wedge initiates as a

horseshoe type vortex pair and after a critical distance additional vortices build up on either side. This process continues until the accumulation of vortices form a turbulence front in the form of a wedge. This structure is similar to that found by Gregory and Walker [5] when looking at the flow downstream of small cylinders using a china clay technique but on a much larger scale.

Fig 9 shows the result for a Mach number of 0.8. In this case there is an interaction of a normal shock with the bubble together with a well developed front of turbulent wedges. The resultant flow pattern is very complex, indicating vortical structures in the broken-up bubble region. Subtle changes of colour in this region varying through red, orange, yellow and green were seen illustrating the complexity of the shear stress distribution.

#### 4.2.2 Swept wing - transition free

A symmetrical wing of 5.5% thick section with a  $55^\circ$  swept leading edge was tested at various speeds. A matt-black stove-enamel finish was applied to the surface. A shear-stress only liquid crystal was sprayed onto the surface and the surface immediately displayed a rich copper-red colour shown in Fig 10. It would seem that this surface finish in some way matched the helical structures in the liquid crystal so that they were aligned into a Grandjean texture. In addition it seems that there is better adhesion of the crystals to the surface.

Fig 11a illustrates the onset of transition for  $M = 0.6$  and  $Re_c^- = 3 \times 10^6$  at zero incidence. The 'scarf' vortex at the wing-body junction shown in the figure as a dark region (but green in colour), merges with another dark region near the trailing edge where the flow is turbulent. The green of these regions contrasts with the orange colour of the laminar flow further upstream. A turbulent wedge has formed near the leading edge. With a change of incidence to  $\alpha = -2^\circ$  (the surface viewed being the upper surface) the transition front moves forward and a series of sharp spikes of transition is apparent in Fig 11b, (observed as green).

Extending the speed range to near the maximum for the wind tunnel, it is possible to obtain a Mach number of 1.2 at about the same mean chord Reynolds number as for the previous case. Results are shown in Fig 12. This model is rather large for the tunnel and, as a result, shock waves reflected from the wall interact with flow on the adjacent model surface. It was observed that the red (low shear stress) region at the  $\lambda$  foot of the shock was oscillatory in a streamwise direction at a frequency of approximately 2 Hz. A still photograph is shown in Fig 12a for results at  $\alpha = 0^\circ$ . The shock wave oscillations are

easily detected since the red low shear stress region contrasts with the green regions immediately upstream and downstream. At about three-quarter span the main shock appears to have caused the flow to separate. The surface as a whole appears as a mottled patchwork of subtle changes of reds and greens with some sharp dividing lines suggesting shocklets emanating from the leading edge. As with the results at  $M = 0.6$ , a small change of incidence to  $\alpha = -2^\circ$  causes transition to occur and advance from the trailing edge as shown in Fig 12b which is a still from the video recording.

#### 4.2.3 Swept fin - transition fixed

An example of the effectiveness of a transition trip has been given in section 4.1. The effect of an alternative form of trip, which offers a consistent method of applying excrescences, is shown in Fig 13. The trip is formed by using the sprocket holes in punched tape as a mould to form a trip consisting of short cylinders of epoxy cement. The cylinders were 1.27 mm diameter and 120  $\mu\text{m}$  in height and spaced at a pitch of 2.54 mm. The test conditions were  $M = 0.3$ ,  $\alpha = 0^\circ$ . Fig 13a shows the onset of turbulent wedges which are widely spaced and merge near the trailing edge at a Reynolds number  $Re_c^- = 1.0 \times 10^6$ . At the transition trip laminar vortices can be seen trailing downstream and persist at least to 25% of the chord. This vortex trail continues into the turbulent region and the only evidence of transition is the dramatic change in colour. With increase of Reynolds number to  $Re_c^- = 1.2 \times 10^6$  the number of wedges has increased five fold (Fig 13b) while further increase to  $Re_c^- = 1.4 \times 10^6$  (Fig 13c) indicates a few remnants of laminar flow just downstream of the transition trip. At  $Re_c^- = 2 \times 10^6$  (Fig 13d) transition appears to be fully fixed although this close-up view clearly shows the strong residual vorticity in the flow. Chan [6] has indicated that this form of transition trip gives favourable results at incidence. It may be that the strong vorticity seen in Fig 13 assists in keeping the boundary layer attached.

#### 4.2.4 Swept wing - isolated roughness

Having shown that liquid crystals can provide fine detail of the flow downstream of transition trips, it was decided to use the technique to investigate the flow downstream of a series of isolated roughness elements. It was hoped that the method might be used to understand more comprehensively the process of transition downstream of roughness elements. Four isolated elements of spherical shape were stuck onto the model at intervals along the 10% chord line

(470 mm in total length). Starting with the most inboard sphere, the diameters were 2.54, 1.27, 0.64 and 0.32 mm. Further outboard were placed a short row of the cylindrical trips, previously discussed in Section 4.2.3.

Fig 14 shows visualisations obtained for  $M = 0.57$ ,  $\alpha = 0$  and  $Re_c = 1 \times 10^6$ . A striking feature here shows the most outboard sphere developing a horse-shoe type vortex pair which continues downstream for approximately a further 20% chord before developing parallel neighbours to form the conventional wedge outline. The most outboard cylinder also shows this effect but its parallel neighbours begin earlier at approximately 10% chord downstream of the trip. Flow lines can be clearly seen running through both the laminar and turbulent areas. Fig 14a shows that all the spherical excrescences created flow disturbances along with the most outboard half of the cylinders. A close-up of the outboard region is illustrated in Fig 14b and an enlargement of the inboard region is shown in Fig 14c. The latter figure shows a pronounced upstream and lateral influence on the flow ( $\approx 6$  times sphere diameter) of the largest sphere with a noticeable diminution of the width (or necking) of the wake just downstream of it. Flows of this type were observed on circular cylinders using a layer of smoke by Gregory and Walker [5] employing a larger scale experiment than the one described in this paper. The fact that such minute flow detail has been visualised in the present experiment argues well the case for using liquid crystals.

##### 5. QUANTITATIVE ASPECTS

In order to determine quantitative shear stress data from the colours of the deformed crystals, a video digitisation technique is being developed at Surrey University. This system involves decoding the light intensity levels for each of the three colour guns in the video camera so that the red (R), green (G) and blue (B) content of the image is known. An example of the response of the three camera guns through the colour spectrum is shown in Fig 15a. By suitable manipulation of this information, the wavelength of light  $\lambda$  may be expressed by a relationship such as that shown in Fig 15b with the condition that contributions of the red and blue components cannot exist together for pure colours with unique values of wavelength  $\lambda$ .

In addition, a calibration is required relating the shear stress  $\tau$  with wavelength  $\lambda$ . Previous attempts to calibrate liquid crystals for shear stress using a rotating viscometer [7] were not completely satisfactory. RAE have made some provisional measurements using a skin friction balance mounted in

the roof of the 2ft x 1½ft Transonic Wind Tunnel by observing the colour changes of the liquid crystals on the surface together with the skin friction reading for a range of Reynolds number. Since the viewing angle is an important parameter the liquid crystals on the balance plate were viewed normally by means of a mirror mounted on the floor of the tunnel. This image is reflected to the cameras by means of a second mirror mounted at a suitable angle at the junction of the tunnel roof and the far sidewall (see Fig 3). The form of an initial calibration is shown in Fig 16 where  $\lambda$  has been determined from a relationship similar to that shown in Fig 15b.

The block diagram of the video digitisation system is shown in Fig 17. It is based on a PDP-11/73 minicomputer, linked by a Q-Bus to digital imaging hardware. Images are provided by either a colour camera in real-time or from pre-recorded video cassettes. True-colour video digitisation is achieved via an Imaging Technology RGB-512 module which is integrated with three frame buffer modules (FB-512) to enable rapid image analysis. The RGB-512 board accepts only separate red, green and blue (R, G, B) video component signals, these being achieved by decoding a standard PAL composite video signal using an Electrocraft PD-84 PAL video decoder unit.

The minicomputer software routines may be used to digitise and store an image in the frame buffers, such that the R, G, B components of each pixel are available for analysis. Any zoomed rectangular portion of the image can then be examined to determine the light wavelength of the pixels.

A preliminary analysis has been made of the flow over the swept wing for  $M = 0.9$  and  $Re_c = 3 \times 10^6$ . The flow is illustrated in Fig 18a and the window area is indicated. The area investigated includes a region of green just downstream of the leading edge changing to orange in the mid-chord region. Natural transition occurs near the trailing edge indicated by spikes of turbulence (green). Digitisation of this data allows the determination of the wavelength corresponding to the pixel colours. Fig 18b shows pixel images of the wavelength  $\lambda$  for the larger part of the window. False colours have been given to the originals to enhance the contrast. Provisional results for the shear stress distribution is shown in Fig 19.

## 6. DISCUSSION

The use of liquid crystals on wind-tunnel models has been shown to be effective in demonstrating the transition process and in illustrating the

ability to sense the complex variations in shear stress which may occur over some surfaces. There has been a learning process and attention needs to be given to many factors.

Since the present interest is directed towards the use of shear sensitive mixtures, which are unsealed, degradation of the liquid crystal is always a possibility [3] but with care this is not considered a problem. Cleanliness aside, the colour play response can be affected by the use of a solvent and colour degradation can result. The finish of the black painted surface may also influence the colour response as well as affecting the adhesion of the liquid crystals to the surface. A 'silk' grade black paint or stove enamel has been found to give good results. Most paints are softened by the solvent used to spray on the liquid crystal and seem to absorb the liquid crystal. A matt black stove-enamelled surface has been found effective in resisting the solvent attack: the process requires heating the surface to 140°C which is not convenient for most wind-tunnel tests. However, carefully painting the liquid crystal on to the surface with a fine camel-hair brush has proved to be completely satisfactory, producing bright unadulterated colours.

For optimum results, the lighting and viewing angles need to be carefully selected. It is usual to view the model perpendicularly and to adjust the lighting position to give maximum colour response without producing glare on the model surface. It may be better to use more than one light source so that, in effect, different parts of the model are illuminated from different angles in such a way as to minimise glare. This procedure is obviously simplified if the liquid crystal on the model surface has been activated into the Grandjean texture.

For the quantitative measurement of shear stress a self consistent testing, calibration and analysis procedure needs to be followed. The response of the three colour guns in the camera needs to be the same as that for the shear stress calibration. The viewing angle also must be taken into account and allowed for on contoured models.

The main advantage over alternative methods of flow visualisation is the ability to provide a continuous assessment of surface flow conditions such as transition without any special modification to the model other than painting the surface. This compares favourably with thermal imaging processes which require thermally insulated surfaces to produce satisfactory images. Sublimation techniques, while often producing some detailed structure of the flow, are 'one-off'

exercises and the procedure needs to be repeated for different flow conditions. Oil flows generally fall into this latter category. Liquid crystals appear to be unique since they are capable of detecting and quantifying shear stress with the added advantage of reversibility.

## 7. CONCLUSIONS

Liquid crystals have been shown to be effective when painted onto a model surface for the on-line visualisation of transition. Utilising their sensitivity to shear stress, wedges of turbulence are clearly defined and the technique provides a rapid means of determining the conditions at which a transition trip on a model is effective.

The fine detail of natural and forced transition is clearly seen and the structure of the transition process is indicated by the initiation of a horse-shoe type vortex which triggers additional vortices on either side.

A scheme has been developed to determine quantitative values for the shear stress using a video digitisation process to produce skin friction contours over a model surface.

REFERENCES

- | <u>No.</u> | <u>Author</u>  | <u>Title, etc</u>   |
|------------|--|---|
| 1          | B.J. Holmes<br>C.G. Croom<br>P.D. Gall<br>G.S. Manuel<br>D.L. Carraway | Advanced transition measurements for flight applications.<br>AIAA-86-Q786 (1986)  |
| 2          | M. Parsley   | BDH Thermochromic Liquid Crystals. A publication of BDH Ltd, UK (1987)  |
| 3          | M. Parsley   | The use of thermochromic liquid crystals in heat transfer and flow visualisation research, 2nd Int. Sympm on fluid-control, measurement, mechanics and flow visualisation: Sheffield, UK (1988) |
| 4          | P.T. Ireland,<br>T.V. Jones  | The measurement of local heat transfer coefficients in blade cooling geometries.<br>AGARD-CP-390 (1985)   |
| 5          | N. Gregory<br>W.S. Walker  | The effect on transition of isolated surface excrescences in the boundary layer.<br>ARC R & M 2779 (1951)   |
| 6          | Y.Y. Chan  | Comparison of boundary layer trips of disc and grit types on aerofoil performance at transonic speeds.<br>NRC, Canada, NAC No 29908 (1988)  |
| 7          | E.J. Klein<br>A.P. Margozzi  | Apparatus for the calibration of shear sensitive liquid crystals.<br>Rev Sci Instrum, 41, 238-239 (1970)  |

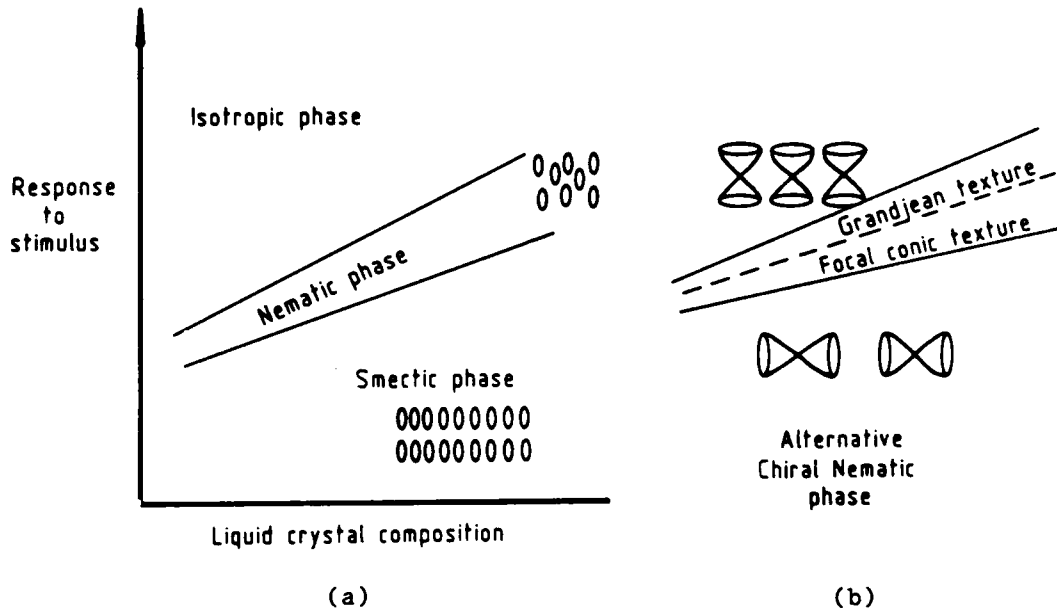


Fig 1 Liquid crystal phase diagram

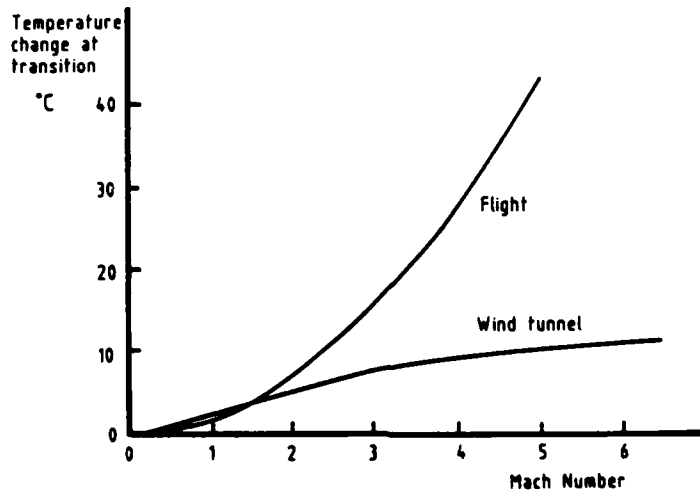


Fig 2 Temperature change at transition with Mach number for flight and wind tunnel

Figs 3&4

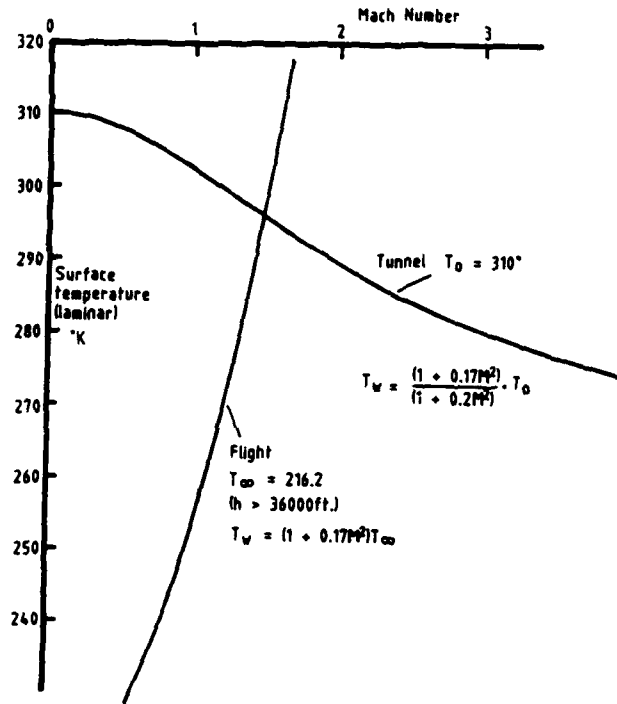


Fig 3 Surface temperature change with Mach number for flight and wind tunnel

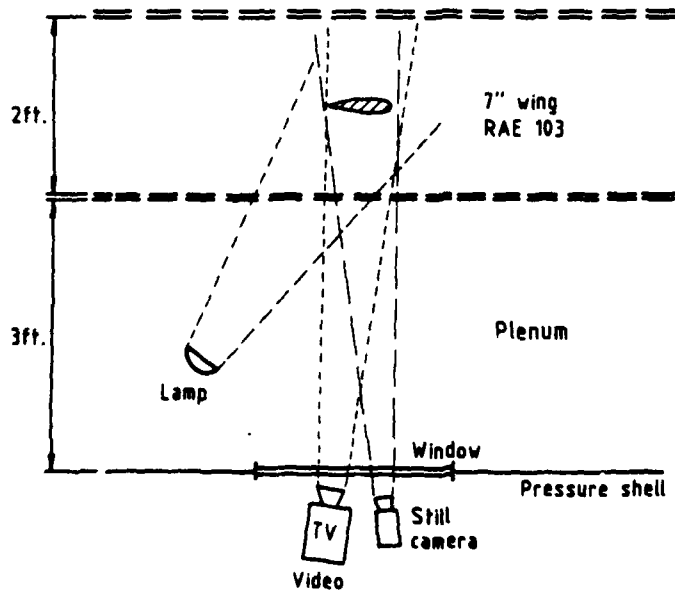


Fig 4 Arrangement in the 2ft x 1½ft Wind Tunnel

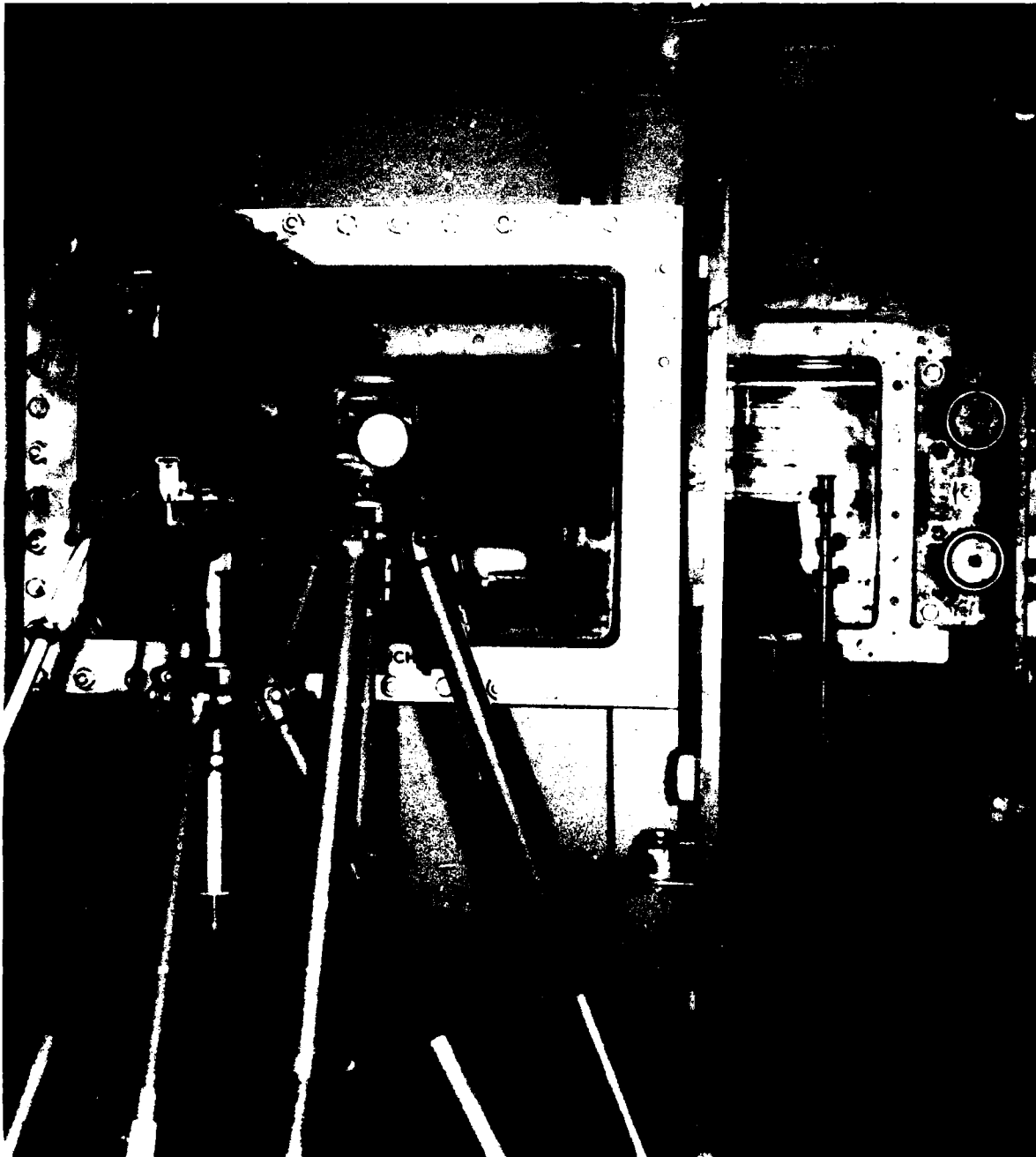


Fig 5 Experimental rig in the  
2ft x 1½ft Wind Tunnel

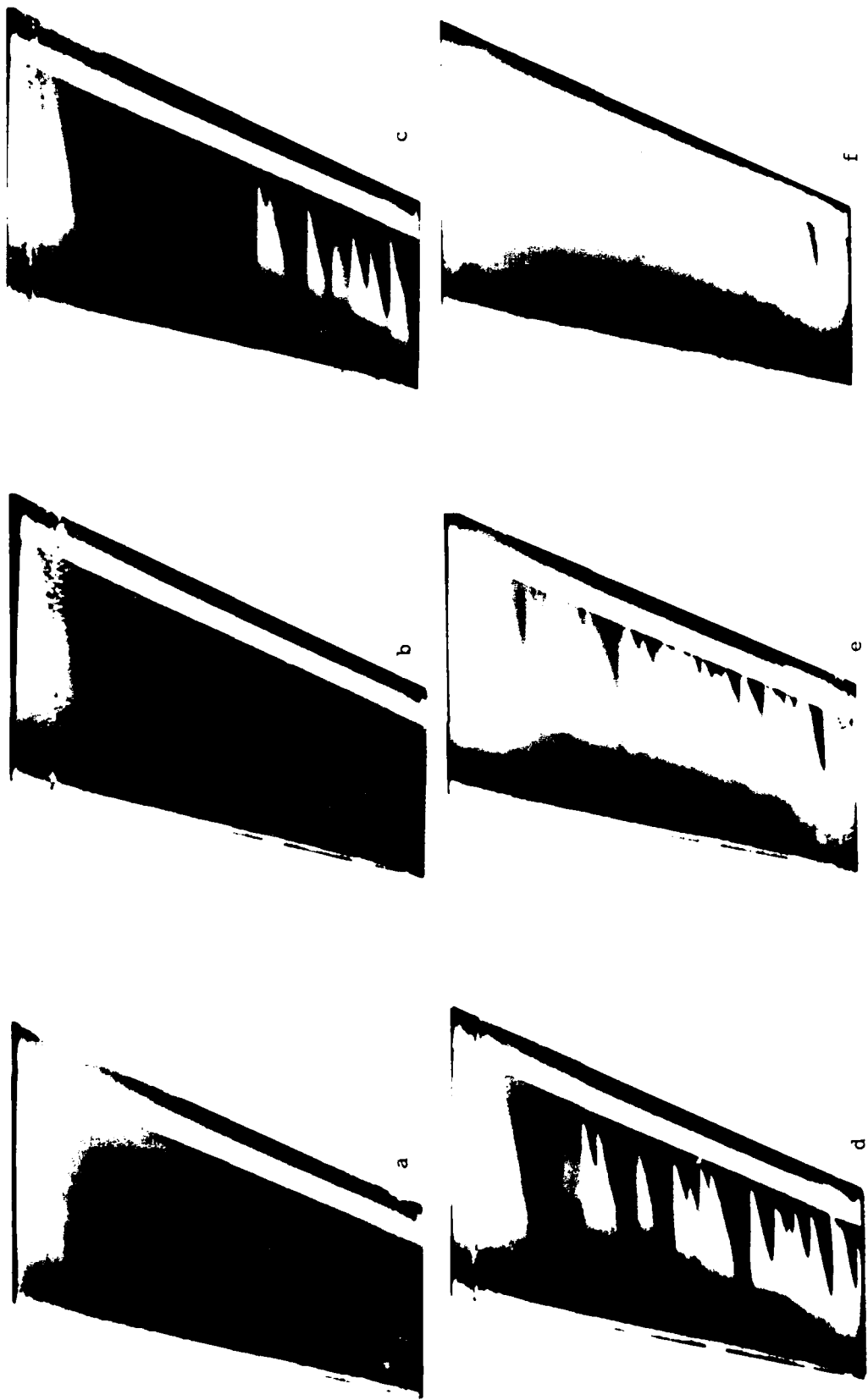


Fig 6 Effectiveness of transition trip with Reynolds number  $M \approx 0.2$

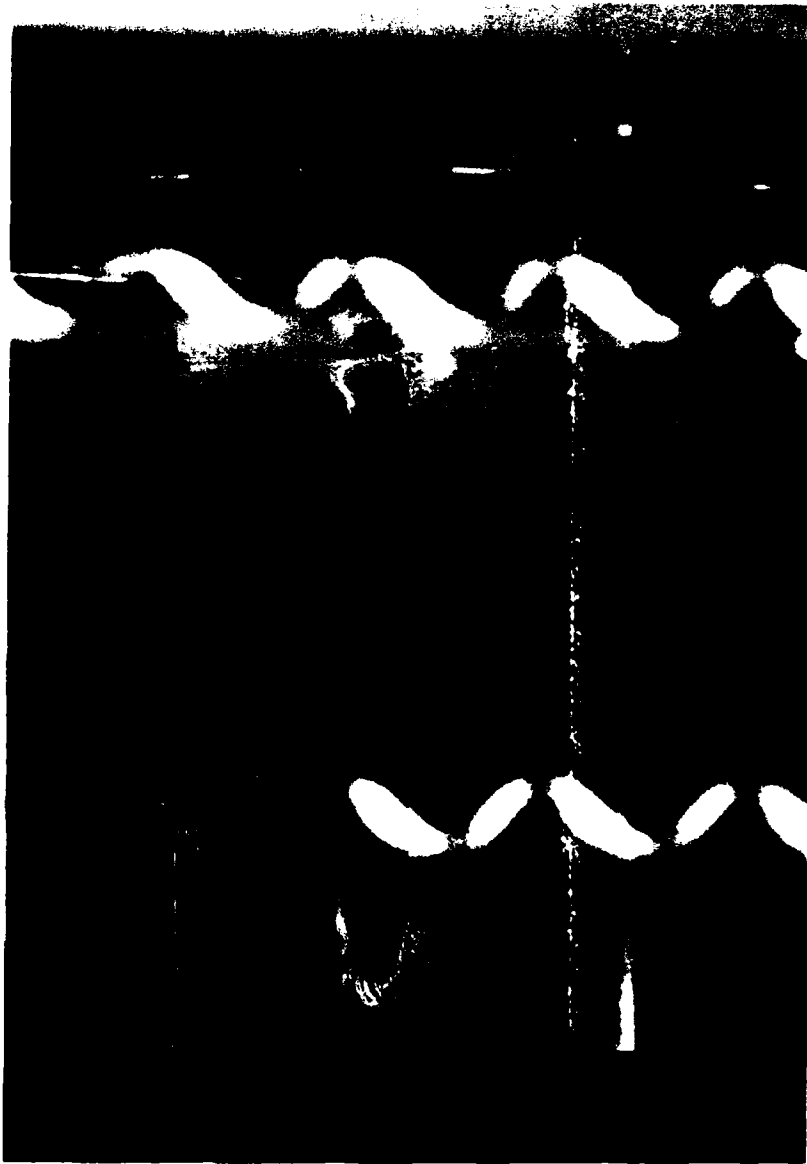


Fig 7 Laminar separation bubble  
on stub wing



Fig 8a Transition wedges with remnants of laminar separation bubble



Fig 8b Enlargement of "a" showing turbulent wedge construction



Fig 9 Stub wing  $M = 0.8$



Fig 10 Wind-off view following initial application of T1511 shear sensitive liquid crystal

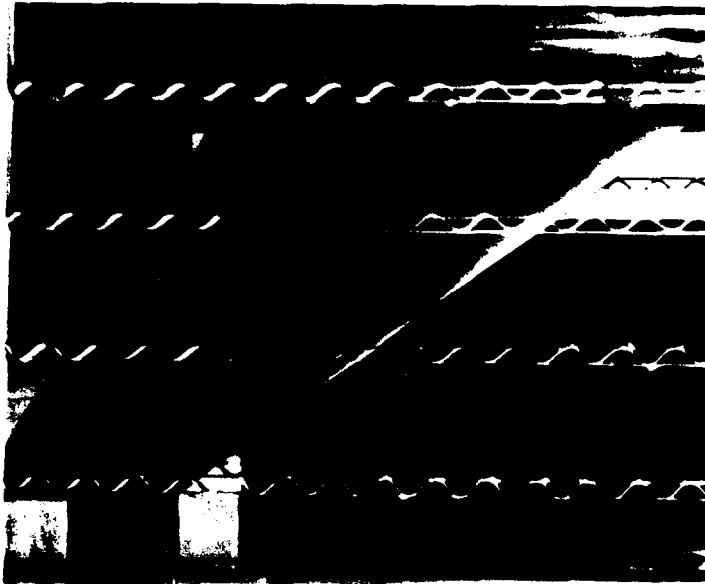


Fig 11a Natural transition plus incidental wedge  $M = 0.6$ ,  $\alpha = 0^\circ$ ,  $Re_c \approx 3 \times 10^6$



Fig 11b Natural transition front moving upstream with change of incidence  $M = 0.6$ ,  $\alpha = -2^\circ$ ,  $Re_c \approx 3 \times 10^6$



Fig 12a Oscillating shock  $M = 1.2$ ,  
 $\alpha = 0^\circ$ ,  $Re_c \approx 3 \times 10^6$



Fig 12b Natural transition front moves  
upstream with change of incidence  
 $M = 1.2$ ,  $\alpha = -2^\circ$ ,  $Re_c \approx 3 \times 10^6$

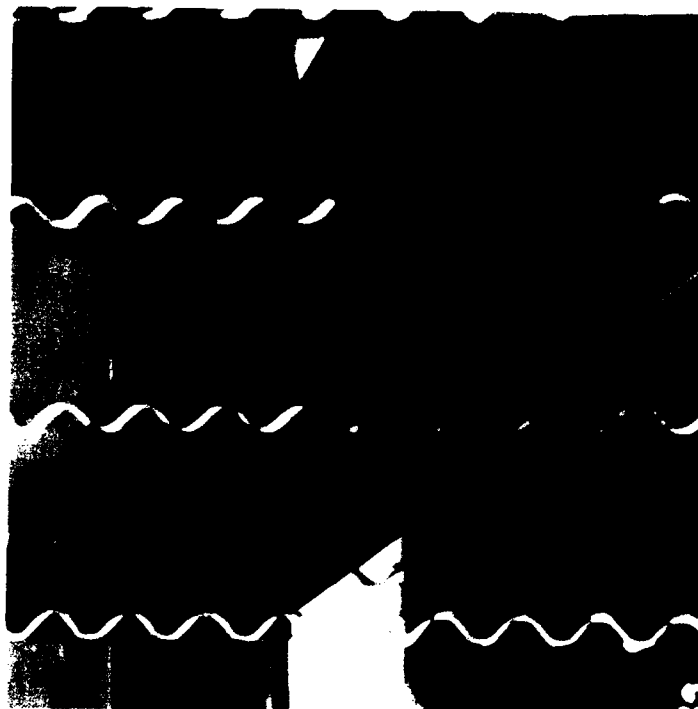


Fig 13a Cylinder-trip showing regular spacing of wedges  $M = 0.3$ ,  $\alpha = 0^\circ$ ,  $Re_c = 1 \times 10^6$

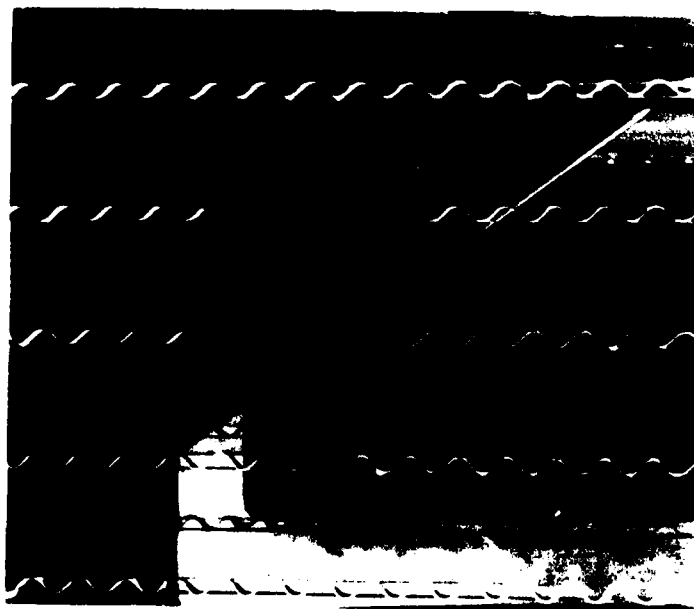


Fig 13b Cylinder-trip showing wedges increasing with Reynolds number  $M = 0.3$ ,  $\alpha = 0^\circ$ ,  $Re_c = 1.2 \times 10^6$

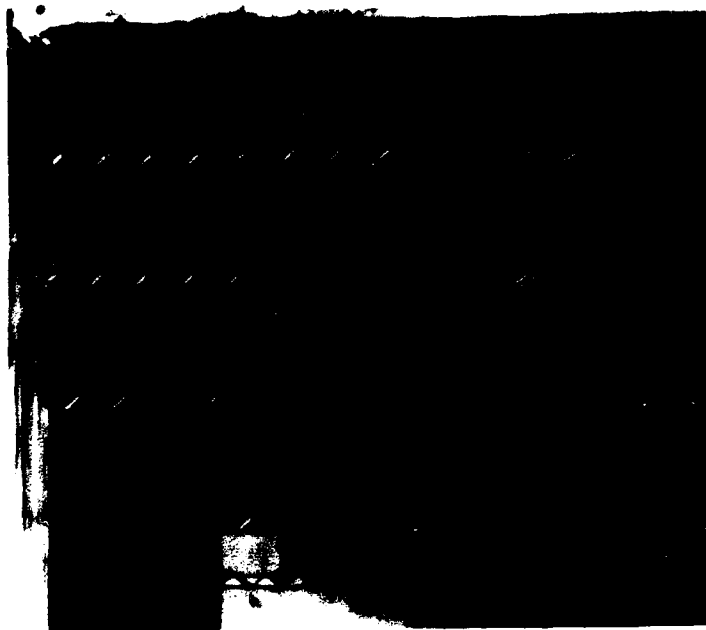


Fig 13c Cylinder-trip showing further increase in number of wedges with Reynolds number  $M = 0.3$ ,  $\alpha = 0^\circ$ ,  $Re_c = 2 \times 10^6$



Fig 13d Cylinder-trip close up showing fully fixed transition  $M = 0.3$ ,  $\alpha = 0^\circ$ ,  $Re_c = 2 \times 10^6$



Fig 14a General view of isolated roughness  
on swept wing showing five spaced  
trips  $M = 0.57$ ,  $\alpha = 0^\circ$ ,  $Re_c = 1.0 \times 10^6$

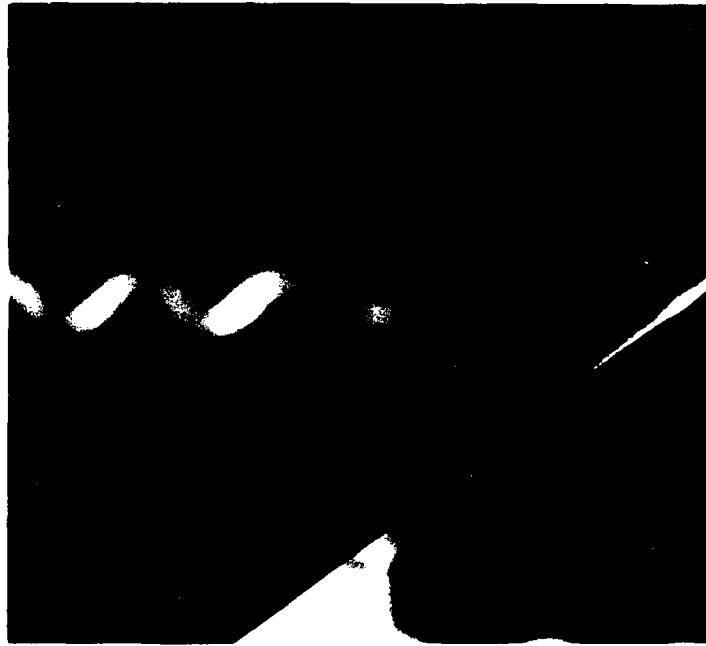
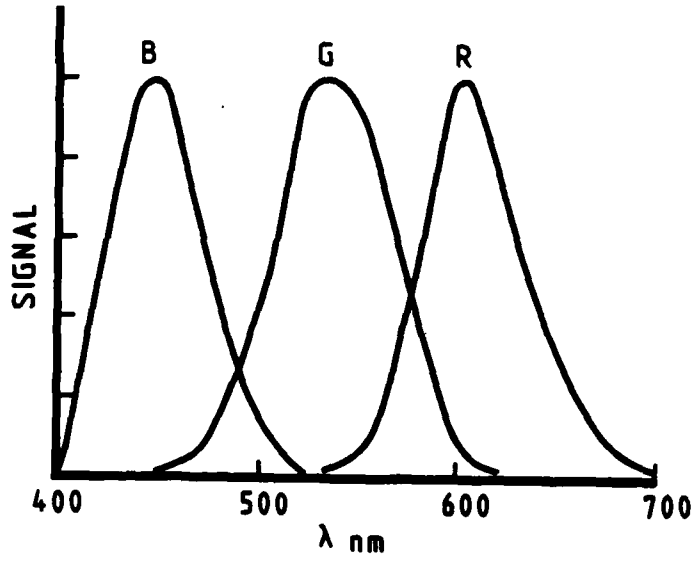


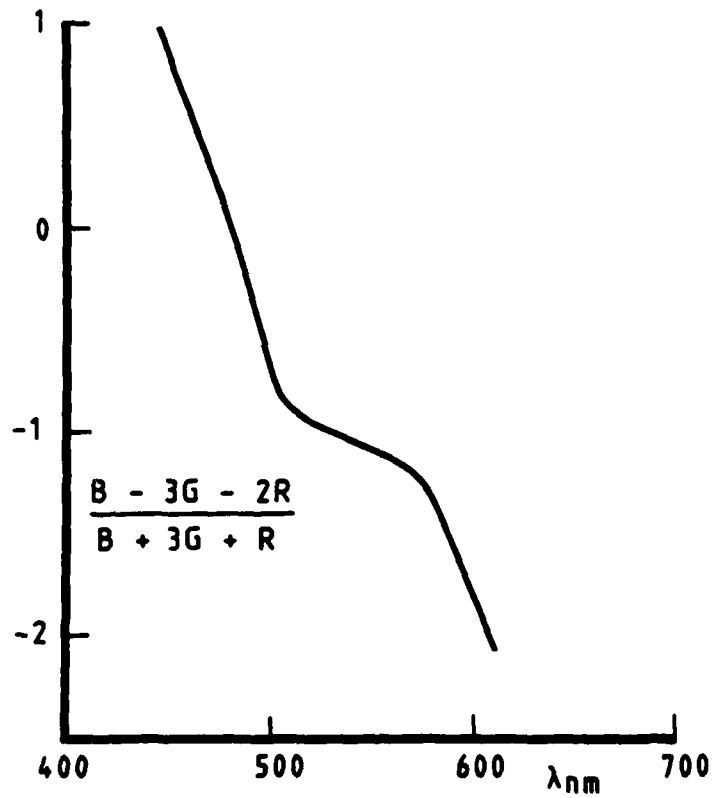
Fig 14b Outboard close-up showing horse-shoe-type vortex pair



Fig 14c Inboard close-up showing field of influence of spheres



(a) Relationship of primary colours with wavelength



(b) Relationship of camera output with wavelength

Fig 15 Typical relationships between colours, camera and wavelength

Figs 16&17

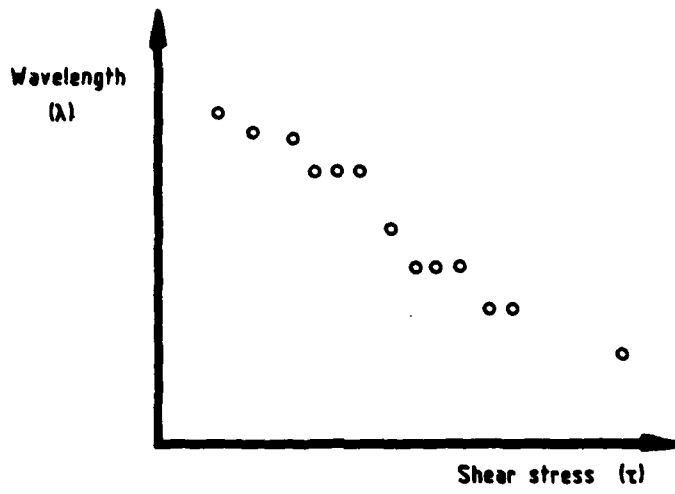


Fig 16 Relationship between shear stress and wavelength

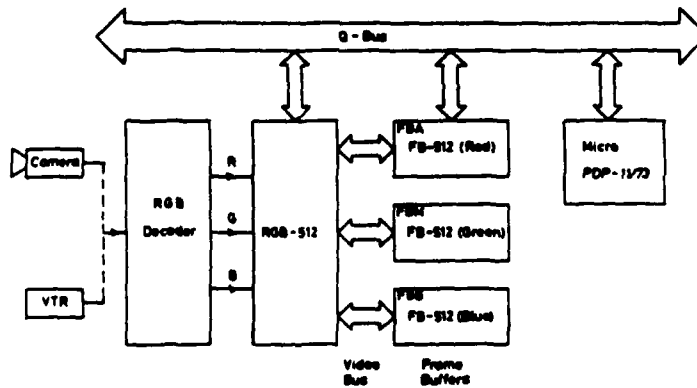
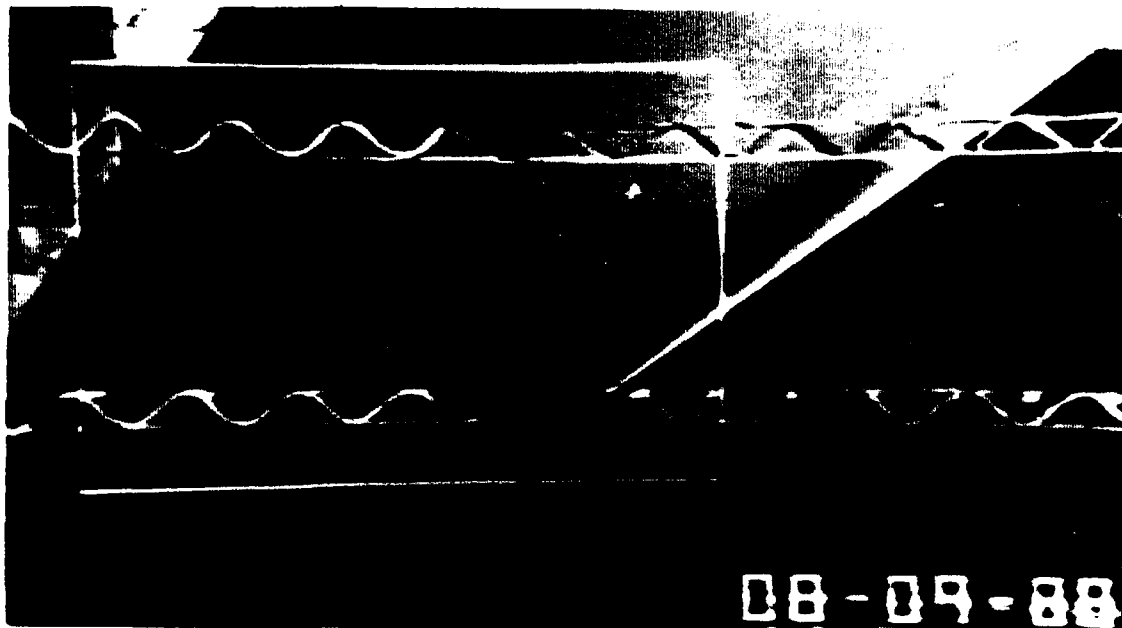
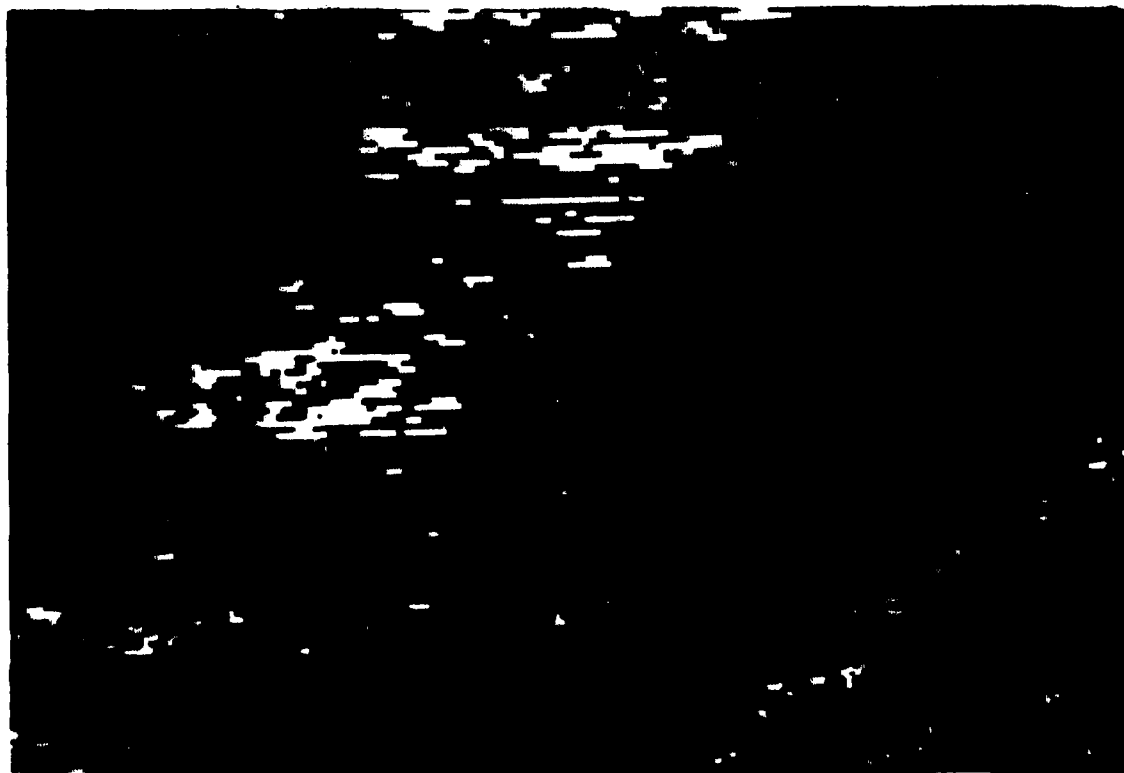


Fig 17 Block diagram of colour video digitisation facility



(a) Surface-flow window position



(b) Pixel images within the surface-flow window

Fig 18 Shear stress measurement on swept wing

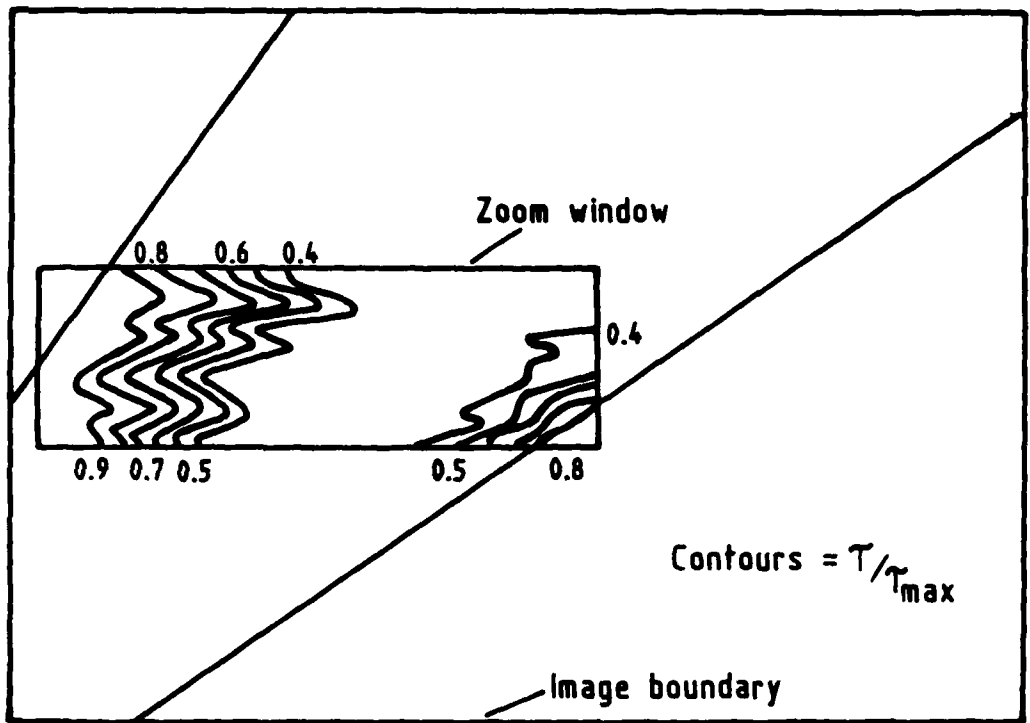


Fig 19 Contours of shear-stress within zoomed window

REPORT DOCUMENTATION PAGE

Overall security classification of this page:

UNLIMITED

As far as possible this page should contain only unclassified information. If it is necessary to enter classified information, the text above must be marked to indicate the classification, e.g. Restricted, Confidential or Secret.

1. DRIC Reference (to be added by DRIC)	2. Originator's Reference RAE TM AERO 2159	3. Agency Reference N/A	4. Report Security Classification/Marking UNLIMITED
5. DRIC Code for Originator 7672000H	6. Originator (Corporate Author) Name and Location Royal Aerospace Establishment, Bedford, Beds, UK		
5a. Sponsoring Agency's Code N/A	6a. Sponsoring Agency (Contract Authority) Name and Location N/A		
7. Title Use of liquid crystals for qualitative and quantitative 2-D studies of transition and skin friction			
7a. (For Translations) Title in Foreign Language			
7b. (For Conference Papers) Title, Place and Date of Conference ICIASF '89 DLR Göttingen September 1989			
8. Author 1. Surname, Initials Gaudet, L.	9a. Author 2 Gell, T. G.	9b. Authors 3, 4 ....	10. Date   Pages   Refs. June 1989   34   7
11. Contract Number N/A	12. Period N/A	13. Project N/A	14. Other Reference Nos.
15. Distribution statement (a) Controlled by – (b) Special limitations (if any) – If it is intended that a copy of this document shall be released overseas refer to RAE Leaflet No.3 to Supplement 6 of MOD Manual 4.			
16. Descriptors (Keywords) (Descriptors marked * are selected from TEST) Liquid Crystals. Flow visualisation. Transition. Skin Friction. Shear stress.			
17. Abstract The exploitation of properties of liquid crystals for use in wind tunnels to visualise transition and to measure skin friction is described. The effectiveness of a transition band to trip the laminar boundary layer on a swept wing is demonstrated by the growth of turbulent wedges with Reynolds number.  The ability of liquid crystals to reveal intricate surface flow structure is clearly shown by subtle changes of colour on an unswept rectangular wing when subjected to the combined effects of transition, separation, reattachment and a normal shock. The time response of liquid crystals to changes in shear stress is illustrated by the shock pattern on the model surface which was seen to be oscillating.  A method involving the digitisation of the video image into its three component colours has the potential for measuring skin friction in great detail. This involves using relationships firstly correlating the component colours with wavelength and secondly correlating shear stress with wavelength.			

ES9101